Time and temperature effects on the behaviour of geosynthetics-reinforced walls

G. Gottardi
Distart, University of Bologna, Bologna, Italy

P. Simonini
Image, University of Padova, Padova, Italy

Keywords: Walls, Reinforcement, Geogrids, Model tests, Laboratory research

ABSTRACT: The research presented in the paper is concerned with the time-dependent response of retaining walls reinforced with polypropylene geogrids and subjected to loads applied at the surface behind the wall. To this purpose a small-scale 1g physical model of geogrid-reinforced wall has been recently built up at the Soil Mechanics Laboratory of the University of Padova. The model tests have been carried out with the main aim of investigating the effects of time and temperature on the subsequent delayed response of reinforced wall. The paper, besides a presentation of the experimental equipment and testing procedure, discusses the results of the experimental programme carried out so far and proposes their analytical interpretation through a simple equation that is capable to describe the long-term behavior of the wall.

1 INTRODUCTION

The use of geosynthetics as reinforcing elements in the construction of walls has greatly increased in the recent years.
The design of such systems requires the knowledge of the mechanical behavior of the system when subjected to various loading conditions, not only at the end of the construction stage but also during the estimated life.
Reduced scale physical models represent a useful mean to analyze such behavior. Examples of experimental investigations carried out in the past using small scale 1g-models of typical walls reinforced with metallic strips can be found in the literature (e.g. Schlosser and Juran, 1983).
The recent introduction of suitable reinforcing elements such as geosynthetics required new experimental work. Several industrial products - geotextiles and geogrids - made of different polymers (polyester, polypropylene, polyethylene) have been produced since 1970. However, laboratory model studies on the behavior of geosynthetics-reinforced walls have been relatively limited. Experiments have been carried out by Juran & Christopher (1989), Tatsuoka et al. (1989), Gourc et al. (1990), Palmeira & Lanz (1994) and Gomes et al. (1994).
One of the most interesting aspects, recently considered by some researchers (Helwany & Wu, 1995; Karpurapu & Bathurst, 1995), concerns the study of the wall long-term behaviour. In fact, it is recognised that geosynthetic materials show time-dependent behaviour, which is influenced by many factors, the most important being the type of polymer, the structure of geo-synthetic, the stress level, the temperature (e.g. Allen, 1991) and the confinements given by the surrounding soil (e.g. Mc Gown et al. 1995; Chang et al., 1996). The delayed deformation is particularly important when the material forming the reinforcement is polypropylene, often used to produce various types of geotextiles and geogrids.
In order to analyze the time dependent behaviour of geosynthetic-reinforced walls a new experimental research has been undertaken at the University of Padova (Italy), concerning the time response of a model wall reinforced with polyethylene geogrids and subjected to surface loads lo-

cated just behind the top of the wall. In this research, due to the creeping nature of the polypropylene geogrids used as reinforcements, the experimental study was especially aimed at the investigation on the long-term behavior of the reinforced structure and its dependence on the temperature level.

2 THE MODEL WALL

The physical model (1200 mm long, 400 mm wide and 600 mm high) intends to reproduce a plain strain state within the rein-forced soil mass. Figure 1 shows a general view of the small-scale model, where the main components - lateral walls, facing elements, reinforced soil and loading plate - can be observed.
The retaining wall is made up of a set of rigid metallic strips, hinged each other and kept vertically only by the interposition of the geogrid layers. The geogrid (1200 mm long and 400 mm wide) are locked into the facing strips and spaced 70 mm. The wall is constructed from the bottom to the top by anchoring the metallic strips to a provisional vertical track, which is removed after the wall construction is completed.

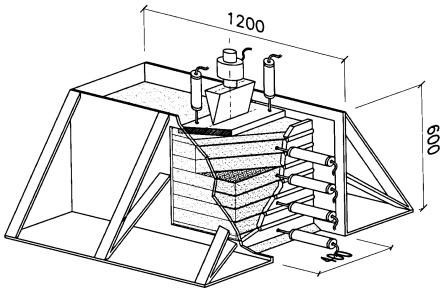

Figure 1. View of the model wall.

The sand layers are prepared by raining technique. All mechanisms for sand deposition are fully automatic and allow for the achievement of homogeneous and highly reproducible layers, the standard deviation of relative density equal to 85% of the layers being less than 1%.
The soil-reinforced retaining wall is loaded, through a rigid steel plate (200 mm x 400 mm) resting on the sand surface, by an electrical stepper motor. The load or displacement path generation and the data acquisition from all measurement devices are fully automatic via a personal computer and an A/D inter-face. The selected position of the displacement transducers al-lows for the continuous monitoring of the lateral displacements of the wall and the vertical displacement and rotation of the plate. A general layout of the physical model is given in figure 2.

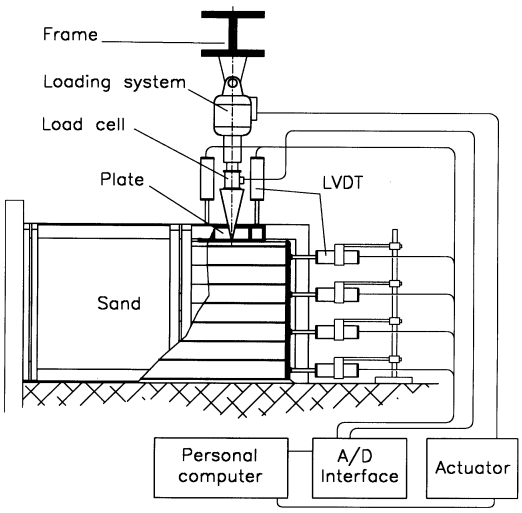

Figure 2. Test lay out.

The material used for soil layer preparation is a medium-fine quartz sand, with mean particle size D_{50}=0.42 mm; non-uniformity coefficient C_u=2.0; specific gravity G_s=2.71, mini-mum and maxi-mum dry unit weight 13.6 e 16.5 kN/m^3. The angle of shear strength, measured from triaxial com-pression tests carried out with the same relative density, is in the range be-tween 41° and 43° under confining stresses ranging from 100 to 400 kPa.
As reinforcing material a suitably scaled polypropylene geogrid was used. It has mesh dimensions of 12 mm x 14 mm and mass per unit area 63 g/m^2. Results of elongation tests are reported in the Figure 2 of a companion paper presented at this conference (Simonini et, al 2000).

3 EXPERIMENTAL PROGRAMME AND TEST RESULTS

The experimental programme was aimed to study the time de-pendent response of the wall when loaded with surface loads. Temperature influence was also accounted for.
To this purpose the wall was subjected to the typical loading paths shown in Figure 3 in the space of the three variables Q, t and w,u where Q is the applied load, t is the time, w and u are re-spectively the vertical displacements of the plate and the horizontal displacements of the wall.
The general loading path is composed by some loading cycles, each of them composed by a ramp loading, a stationary loading and an unloading-reloading (Figure 3). The ramp load was applied using different loading rates in the different tests, via successive 5 KN increments. Each level the load was subsequently kept constant for the remaining time period in order to give a total time equal to $2.5 \cdot 10^5$ seconds. The load was then de-creased of 5 KN, back to the starting value of each load step where it was kept constant for a slightly shorter time. A typical loading cycle is depicted in Figure 4. Each test required a total time - including wall preparation – of about one month.

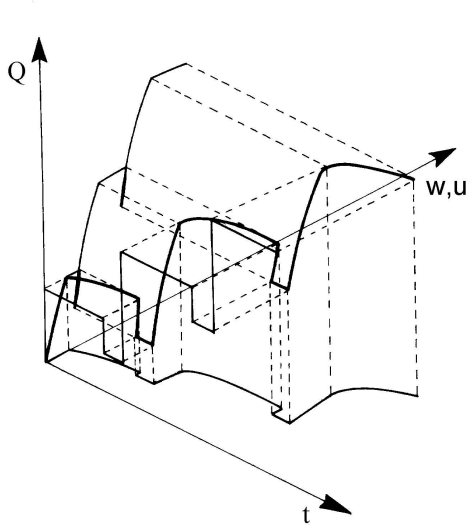

Figure 3. Typical loading path.

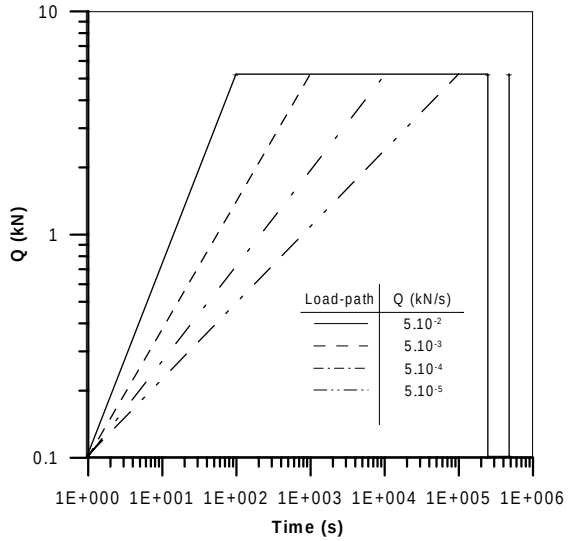

Figure 4. Load-time path for a typical loading cycle.

All the tests were driven up to the failure characterized by the collapse of the reinforced wall due to the progressive break-age of the polymeric grids. Table 1 summarizes the tests carried out so far.

Table 1. Testing program.

Test	Ramp-load time (s)	Constant-load time (s)	Total load time (s)	T (°C)
E2	$1.0 \cdot 10^{2}$	$2.499 \cdot 10^{5}$	$2.5 \cdot 10^{5}$	10
E3	$1.0 \cdot 10^{3}$	$2.490 \cdot 10^{5}$	$2.5 \cdot 10^{5}$	10
E4	$1.0 \cdot 10^{4}$	$2.400 \cdot 10^{5}$	$2.5 \cdot 10^{5}$	10
E5	$1.0 \cdot 10^{5}$	$1.500 \cdot 10^{5}$	$2.5 \cdot 10^{5}$	10
E2T20	$1.0 \cdot 10^{2}$	$2.499 \cdot 10^{5}$	$2.5 \cdot 10^{5}$	20
E2T30	$1.0 \cdot 10^{2}$	$2.499 \cdot 10^{5}$	$2.5 \cdot 10^{5}$	30
E0	-	-	Up to failure	10

Tests labeled E0 and E0T30 are particular reference tests, in which the model was driven to failure with a constant loading rate equal to $5 \cdot 10^{-2}$ kN/s and no interposition of any constant load phase.
The last column of table 1 reports the average temperature of the environment. It ranges from low values (10°C) up to higher values (30°), namely a typical range of temperature excursion in temperate regions.
Figure 5 provides typical results - referred to test E2 at T=10 °C – of the relationship between the applied load Q and the displacements both of the wall (u_3, u_4, u_5, u_6 and M) and of the plate ($(w_1+w_2)/2$). Note the similar trend of the load-displacement curves for all the loading steps, where all the separate different phases can be clearly observed. The load - vertical displacement curve, located at the right of the other curves, is significantly affected by the initial bedding errors of the plate. The other tests showed a similar general trend of the overall load-displacement behavior, but with different values of the actual displacements.
No significant displacement recovery of the reinforced soil was noted after each unloading stage and for all the displacement transducers.

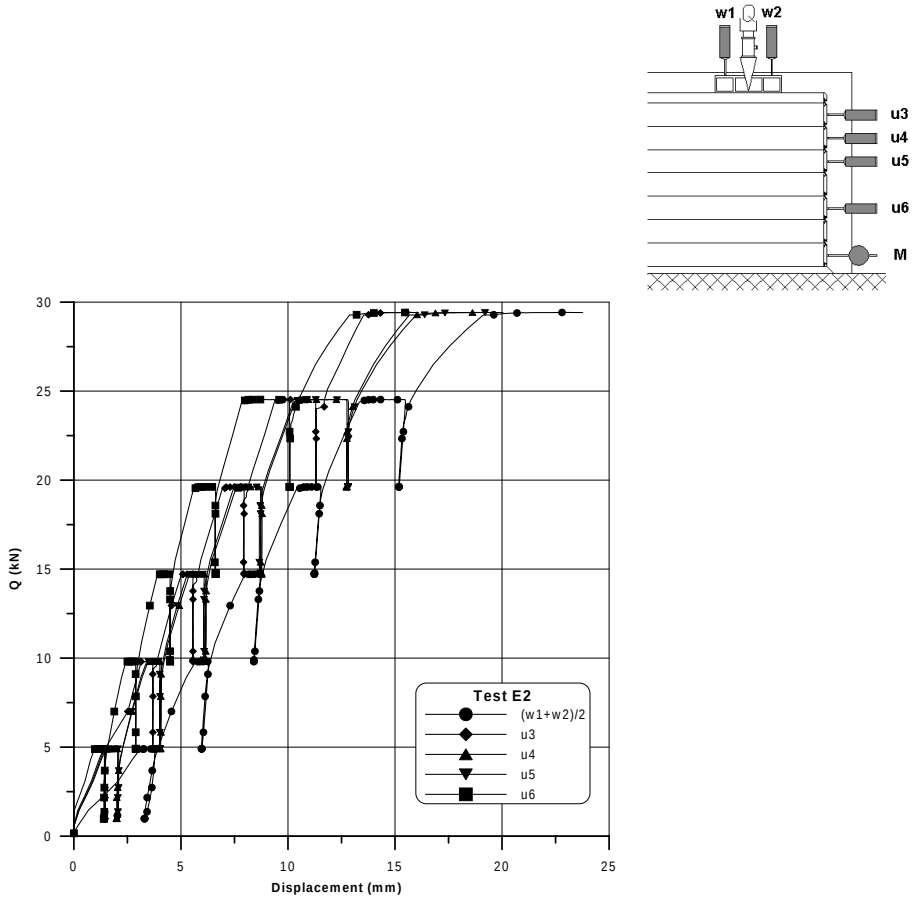

Figure 5. Load-displacement behavior from horizontal and vertical displacement transducers.

Figure 6 shows the deformed sand mass immediately after failure, with the localization of the sliding surface, as deduced from the deformations of a colored sand square grid inserted during the sample preparation (horizontal lines correspond to reinforcements). All reinforcements, but the shallowest, were long enough to be certainly prevented from being pulled out. It is interesting to observe that the position and shape of the failure surface is not too distant from what is usually proposed in the cur-rent design methods, despite the different stress field induced by the surface plate into the reinforced soil mass.

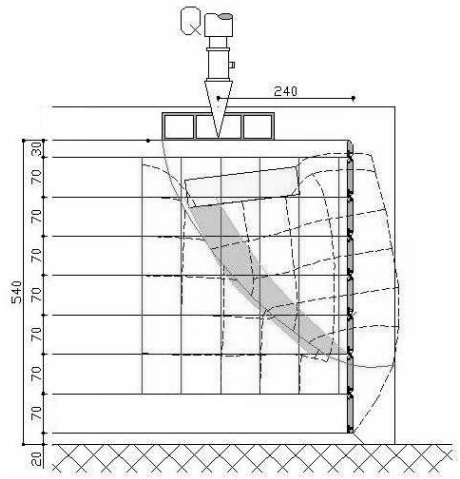

Figure 6. Deformed mesh at failure (test E3).

In this paper we consider only the delayed response of the wall during the constant load phases.
Initially we examine and compare the stationary phases of the tests E2, E3, E4 and E5, carried out with approximately the same temperature of the environment T = 10 °C. Four load levels, namely Q = 0.25, 0.375, 0,50 and 0.625 Q_{max}, are taken into consideration, where Q_{max} = 40 KN is the maximum load determined at failure in the quick reference test E0 performed at a temperature T=10 °C. The first load level, i.e. Q=0.125 Q_{max}, was not considered due to the relevant bedding errors influenc-ing the initial part of the load-displacement curves.
Figure 7 shows the trend of the vertical displacement of the plate $w_s = (w_1+w_2)/2$ as a function of time (t-t_1) and dimensionless load level. Time t_1 is the time at the beginning of the constant load phase ($Q = Q_{const}$). Note that only the plate displacement is considered here in the analysis of the test data, but similar trends were observed for all the horizontal displacements. Therefore our considerations could be easily applied to the analysis of anyone of the horizontal displacements of the wall.
From the experimental data a quite regular trend of the displacement as a function of time turned out. The effect of load level appears to be relatively small almost up to 0.625 Q_{max}, but exceeding this value its influence suddenly becomes particularly important inducing tertiary creep and collapse of the wall (occurred at Q = 0.75 Q_{max} for all the four tests).

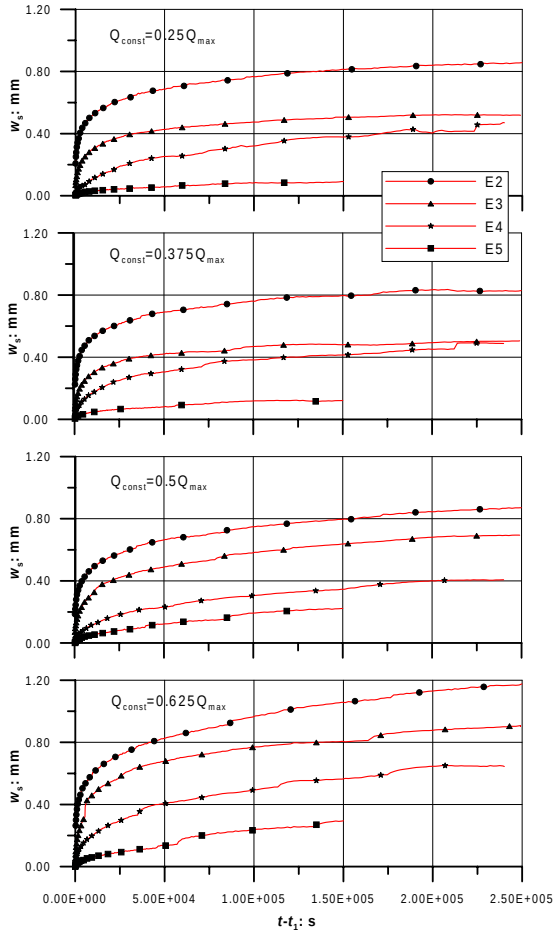

Figure 7. Trends of plate displacement as a function of time and load level during the constant load phase.

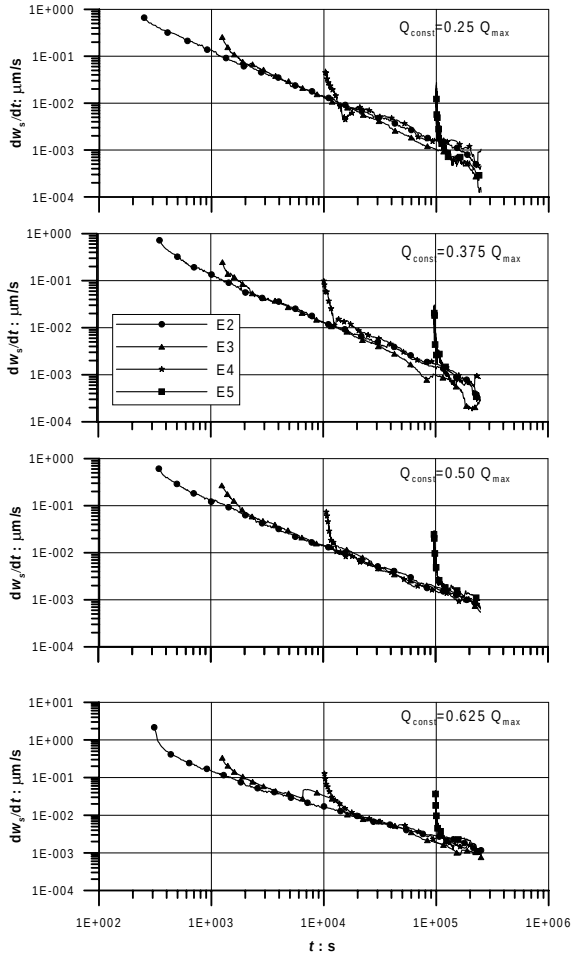

Figure 8. Rate of plate displacement as a function of time and load level during the constant load phase.

However, it is more convenient to perform time-dependent analyses in terms of displacement rate rather than of cumulative displacement. Therefore, in Figure 8, the average vertical dis-placement rate dw_s/dt is plotted against time t (t = 0 seconds at the beginning of each loading cycle). It is interesting to observe that - within the load ranges considered here - the displacement rates dw_s/dt decreases as a function of time. The influence of the previous load-time history on the subsequent response can be noted: when the loading rate is very high the dw_s/dt after t_1 (the time at end of ramp loading phase) occurs at very high rate at the beginning of the constant load phase, but it is soon reduced of two orders of magnitude. However all the displacement rates seem to converge towards a unique general trend for all the tests, characterized approximately by the same slope in the plane (dw_s/dt, t), independently from the previous history.
It is also interesting to consider the influence of the temperature on the response of the wall. To this purpose, the results of tests E2, E2T20 and E2T30 are examined and compared in Figure 9 in terms of displacement rate. Despite the limited number of tests carried out so far, the strong effect of the temperature level on the displacement rate can be noted: at load levels equal to 50% of the maximum value Q_{max} only the wall tested at T=10° C does not reach the failure condition.
From these preliminary results it appears that a relatively small range of temperature – from 10° to 30 ° C – provides so relevant changes of the polypropylene properties to cause the failure of the wall. In other words, a temperature increase could be imagined as a load level increase, but with a stronger effect for the stability of the wall.

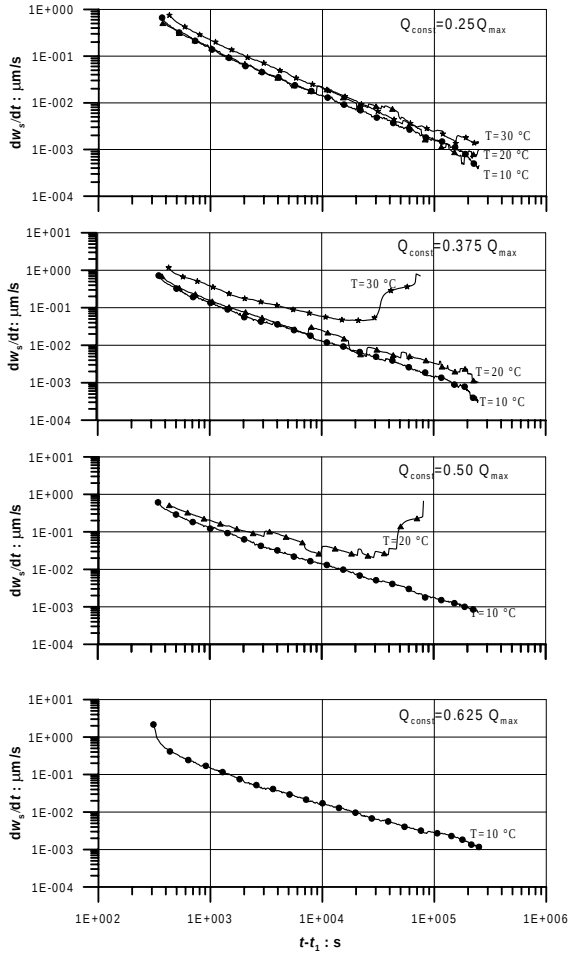

Figure 9. Rate of plate displacement as a function of time and tempera-ture level during the constant load phase.

4 ANALYTICAL INTERPRETATION OF THE TIME-DEPENDENT BEHAVIOR AT CONSTANT TEMPERATURE AND LOAD LEVEL

From the analysis of the overall response of the wall depicted in Figure 5, it can be observed that the general displacement – either vertical of the plate or horizontal of any point along the wall – could be considered as sum of three separate components, which in terms of vertical displacement of the plate, could be therefore expressed as:

$$w_t = w_e + w_p + w_v \tag{1}$$

where wt is the total displacement and w_e, w_p, w_v are, respectively, the elastic, plastic and viscous component of the total displacement.
As pointed out above, the main aim of the present research is to focus the attention on the analysis of the time-dependent com-ponent of the total displacement, and more particularly that at constant load and temperature level.
In order to describe the overall time-dependent response, we could imagine the model wall as a homogeneized continuous element, with no distinction between sand layers and geogrid elements.

It is evident that the viscous response of the reinforced soil is mainly due to the geosynthetics, since the time-dependent deformation of dense sand can be considered as negligible with respect to that provided by the reinforcing elements.
If we suppose to neglect the effect of temperature considering only the influence of load level and time on the wall response, the viscous displacement could be tentatively expressed as follows:

$$w_v = \iint_{Q,t} f(Q,t)\,dQdt \tag{2}$$

where f is a generic function that accounts for the effects of load level (assuming a monotonic loading history) and time on the viscous response of the reinforced soil.
Among the various possible functions f to be used in eq. (2) to describe the time-dependent response of the wall, the following was adopted:

$$f(Q,t) = \frac{dw_v}{dt} = A \cdot e^{aQ} \cdot (t/t_0 - 1)^m \quad for\, Q < Q_{\max}\ and\ t \geq t_0 \tag{3}$$

where A, a and m are experimental parameters. The time t_0 is the reference time at the beginning of the test, taken equal to 1 second.
Such function is similar to the well-known equation proposed by Singh and Mitchell (1968), which has already proved to be adequate for the description of the creep-rate characteristics of a large variety of soils and has also shown to be a powerful tool to model the time-dependent response of some polymeric materials (Simonini, 1998).
During the ramp-loading phase in the model tests, the load is solely a function of time. On the contrary, during the constant-load phase Q = const = Q_1; therefore, the exponential function of eq. (3) is a constant throughout the whole time interval.
Hence we can write:

$$w_v = Ae^{aQ_1} \int_{t_1}^{t_2} (t/t_0 - 1)^m\,dt = \frac{At_0}{m+1} e^{aQ_1} \left((t_2/t_0 - 1)^{m+1} - (t_2/t_0 - 1)^{m+1} \right) \tag{4a}$$

if $m \neq -1$ and if $m = -1$

$$w_v = Ae^{aQ_1} \int_{t_1}^{t_2} (t/t_0 - 1)^m\,dt = At_0 e^{aQ_1} \ln \frac{t_2 - t_0}{t_1 - t_0} \tag{4b}$$

where t_2 is the time at the end of the constant-load phase.
Results from model tests carried out at the same reference temperature level, i.e. T = 10 °C (E2, E3, E4 and E5) and depicted in Figures 7 and 8 were used to calibrate eqs. (4a) or (4b) and determine the relevant experimental parameters. It was assumed $w_s = w_v$.
From the trends reported in Figure 8 it was seen that a round value of m = -1 fits reasonably well the experimental data. In addition, via a least squares regression of the displacement rate at various load levels, the following values of the other experimental constants of eq. (3) were obtained: A = 110 mm/s; a = 0.64; m = -1.
Equation (4b) can therefore be used to predict the delayed response of the plate under constant load.

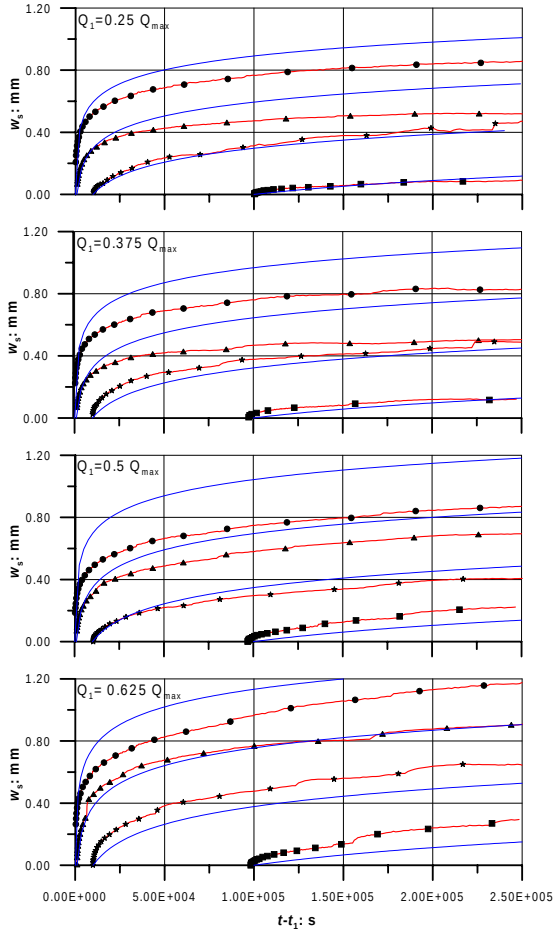

Figure 10. Measured and predicted displacement of the plate (see Fig. 7 for the legend).

In order to check the reliability of eq. (4b) with the above values of the experimental constants, a prediction of displacements during the constant load phases was carried out.
The result is plotted in Figure 10, where the analytical trends are superimposed on the experimental ones. From Figure 10 it appears a substantial agreement between predicted and measured trends of displacement.
It must be bear in mind the relevant difficulty in modeling such complex behaviour via simple methods: however the Singh and Mitchell equation seems to capture the basic creeping response of the wall.

5 CONCLUSIONS

This paper presented and discussed results form the model tests of a polypropylene geogrid-reinforced wall.
The experimental set-up has proved to provide accurate and repeatable test conditions, considering the very complex interaction problem under investigation. In particular, the fully automatic data acquisition and control enabled to carry out long-term tests, in order to study the time-dependent response of the reinforced wall.
From the research presented here, the following main conclusions can be drawn.

The presence of a time-dependent response of the wall due to the creeping nature of polypropylene was clearly observed. The creep rate is influenced by many factors: among these the effect of loading history and load and temperature level was examined. We considered particularly the delayed response of the wall at constant load levels.
It was observed that longer the loading time, smaller the creep rate after the loading phase, i.e. the viscous component of deformation significantly occurs already during the loading phase.
The load level applied behind the wall does not seem to affect significantly the time dependent response of the wall at constant load, almost up to 50% of the maximum load sustainable by the wall.
On the contrary a strong effect of temperature level on overall time-dependent response of the wall was noted: a slight temperature increase could provide relevant changes in the mechanical properties of the polymers, thus causing tertiary creep and col-lapse of the wall.
No relaxation and time-dependent displacement recovery of the reinforced soil was noted during each unloading stage and for all the tests and load levels.
Finally, one of the most interesting remarks is that, during the constant load phases, the displacement rates for all the test and load levels seem to converge towards an unique general trend, independently on the previous loading history. This tentatively suggested an analytical interpretation of test results based on a simple three-parameter equation that seems to be capable of de-scribing with reasonable accuracy the long-term response of the wall. Future research is however needed to corroborate the validity of proposed approach.

ACKNOWLEDGEMENTS

Tenax S.p.A. is kindly acknowledged for providing the geogrids and the relevant data used in this research.

REFERENCES

Allen, T.M., 1991. Determination of long-term tensile strength of geosynthetics: A state of the art review. *Proc. of Geosynthetics '91 Conference*: 351-379. Atlanta, USA.

Chang, D.T.T., Chen, C.A., Fu, Y.C. 1996. The creep behaviour of geotextiles under confined and unconfined conditions. *Proc. of the Int. Symp. on Earth Reinforcement*: 19-24. Fukuoka, Japan.

Gomes, R.C., Palmeira, E.M., Lanz, D. 1994. Failure and deformation mechanisms in model reinforced walls subjected to different loading conditions. *Geosynthetics International,* 1 (No.1): 45-65.

Gourc, J.P., Gotteland, P., Wilson-Jones, H. 1990. Cellular retaining walls renforced by geosynthetics: behaviour and design. *Proc. of the International Reinforced Soil Conference*: 41-45. British Geotechnical Society, Glasgow.

Helwany, M.B., Wu, J.T.H. 1995. A numerical model for analyzing long-term performance of geosynthetic-reinforced soil structures. *Geosynthetics International,* 2 (No.2): 429-453.

Juran, I., Christopher, B. 1989. Laboratory model study on geosynthetic reinforced soil retaining walls. *J. of Geot. Eng., ASCE*, 115 (No.7): 905-926.

Karpurapu, R., Bathurst, R.J. 1995. Behaviour of geosynthetic reinforced soil retaining walls using the finite element method. *Computer and Geotechnics*, 17: 279-299.

Mc Gown, A., Yogarajah, I., Andrawes, K.Z., Saad, M.A. 1995. Strain behaviour of polymeric geogrids subjected to sustained loading in air and soil. *Geosynthetics International,* 2 (No.1): 341-355.

Palmeira, E.M., Lanz, D. 1994. Stresses and deformations in geotextile reinforced model walls. *Geotextiles and Geomembranes*, 13: 331-348.

Schlosser, F., Juran, I. 1983. Behaviour of reinforced earth retaining walls from model studies. *Development of Soil Mechanics: Model Studies, Banerjee and Butterfield eds.* London: Applied Sciences Publisher.

Simonini P. 1998. On the use of viscoplasticity to describe time-dependent behaviour of polyethylene geomembranes. *Soils and Foundations,* 38 (No.4). The Japanese Society for Soil Mechanics and Foundation Engineering.

Simonini, P., Schiavo, M., Gottardi, G., Tonni, L. 2000. Numerical analysis of a model wall reinforced with polypropylene geogrids. *EuroGeo 2000, 2nd Eur. Conf. on Geosynthetics, Bologna.*

Singh, A., Mitchell, J.K. 1968. General stress-strain-time function for soils. *J. of Geot. Eng., ASCE,* 94 (SM1): 21-46.

Tatsuoka, F., Tateyama, M., Murata, O. 1989. Earth retaining wall with a short geotextile and a rigid facing. *Proc. of the 12th Int. Conf. on Soil Mech. and Found. Eng.,* 2: 1311-1314.